Manipulating microwaves with magnetic-dipolar-mode vortices

E. O. Kamenetskii, M. Sigalov, and R. Shavit
Department of Electrical and Computer Engineering, Ben Gurion University of the Negev, IL-84 105 Beer Sheva, Israel
(Received 29 September 2009; revised manuscript received 1 December 2009; published 18 May 2010)

There has been a surge of interest in the subwavelength confinement of electromagnetic fields. It is well known that, in optics, subwavelength confinement can be obtained from surface plasmon (quasielectrostatic) oscillations. In this article, we propose to realize subwavelength confinement in microwaves by using dipolar-mode (quasimagnetostatic) magnon oscillations in ferrite particles. Our studies of interactions between microwave electromagnetic fields and small ferrite particles with magnetic-dipolar-mode (MDM) oscillations show strong localization of electromagnetic energy. MDM oscillations in a ferrite disk are at the origin of topological singularities resulting in Poynting vector vortices and symmetry breakings of the microwave near fields. We show that new subwavelength microwave structures can be realized based on a system of interacting MDM ferrite disks. Wave propagation of electromagnetic signals in such structures is characterized by topological phase variations. Interactions of microwave fields with an MDM ferrite disk and MDM-disk arrays open a perspective for creating engineered electromagnetic fields with unique symmetry properties.

DOI: 10.1103/PhysRevA.81.053823 PACS number(s): 42.25.Fx, 42.30.Va, 76.50.+g

I. INTRODUCTION

Recent studies of magnetic-dipolar interactions in a quasi-two-dimensional (2D) ferrite disk revealed unique properties of eigenmode oscillations. The magnetic-dipolar modes (MDMs) are characterized by energy eigenstates [1,2], gauge electric fluxes, and eigenelectric (anapole) moments [3]. Special vortex characteristics of MDMs in thin-film ferrite disks were found numerically and analytically [4,5]. The results give deep insight into an explanation of the experimental multiresonance absorption spectra shown both in previous [6,7] and new [8–10] studies. It is well known that MDM [or magnetostatic (MS)] resonators fabricated with single-crystal yttrium iron garnet films are open resonators with high Q-factors [11]. In a quasi-2D ferrite disk, one clearly observes regular multiresonance spectra of high-Q-factor MDMs [6–10]. At the same time, MDM oscillations in a ferrite disk are characterized by unique symmetry properties. These symmetry properties may assume peculiar interactions of a ferrite disk with external electromagnetic fields. In this article, we show that, due to the vortex behavior of MDM oscillations, there is strong three-dimensional (3D) localization of electromagnetic energy with the Poynting vector vortices.

For a proper analysis of the Poynting vector vortices and field manipulating in microwaves, one should start with some references to the known phenomena of the Poynting vector vortices and field manipulation in optics. It is very important to note that certain similarities exist between electromagnetic topological singularities at microwave and optical frequencies. The Poynting vector topological singularities are well-studied in optics. It was shown, in particular, that optical beams with phase singularities are robust structures with respect to perturbations. In such beams, one has a circulating flow of energy resulting in 2D confinement of electromagnetic energy in transversal directions [12]. In near-field optics, because of phase singularities one obtains subwavelength transmission through narrow slits [13], novel superlenses [14], and super-resolution processes in metamaterials [15]. The possibility of compressing optical fields in space to a degree much better than predictable by classical diffraction theory has gained widespread attention. For example, the localization of electromagnetic energy is considered as a very important phenomenon for optical sensing and optical data communication. Use of the optical-near-field characterization technique should reduce the size gap between optical and electronic devices [16,17]. It makes it possible to downscale established antenna design into the optical frequency regime [18–20]. In such optical structures, subwavelength confinement of the light takes place because of the resonant interaction between electrostatic oscillations of electrons in metal nanoparticles and planar films and the electromagnetic field. In an analysis of scattered optical electromagnetic fields, a small (with sizes much less than the electromagnetic wavelength) metal particle with plasmonic (electrostatic) oscillations can be treated as a point electric dipole precisely oriented in space [21,22]. It was pointed out that, in small particles with plasmonic resonances, one has anomalous light scattering characterized by giant optical resonances with enhanced scattering cross sections [23].

In this article we show that, similarly to manipulating optical fields by small metal particles with electrostatic (plasmonic) oscillations, one can manipulate microwave fields by small ferrite particles with magnetostatic (magneto-dipole) oscillations. As we show, a small ferrite particle with MDM (or magnetostatic) oscillations has a property of a rotating magnetic dipole. Such particles become “harbors” for the microwave fields. The electromagnetic fields scattered from the MDM particles have very unique symmetry properties and topological structures.

The near-field Poynting vector singularities, appearing due to the interaction of microwave fields with an MDM ferrite disk, open a perspective for creating engineered electromagnetic fields with unique symmetry properties. We show that based on an array of MDM ferrite particles with evanescent-tail chiral coupling, one can realize subwavelength microwave structures with a channeling of topological excitations (channeling of microwave power-flow vortices). The subwavelength confinement and near-field manipulation of the electromagnetic fields is one of the main attractive aspects of the concept of metamaterials, both in optics and in microwaves [24–28]. The unique symmetry properties of a system of interacting

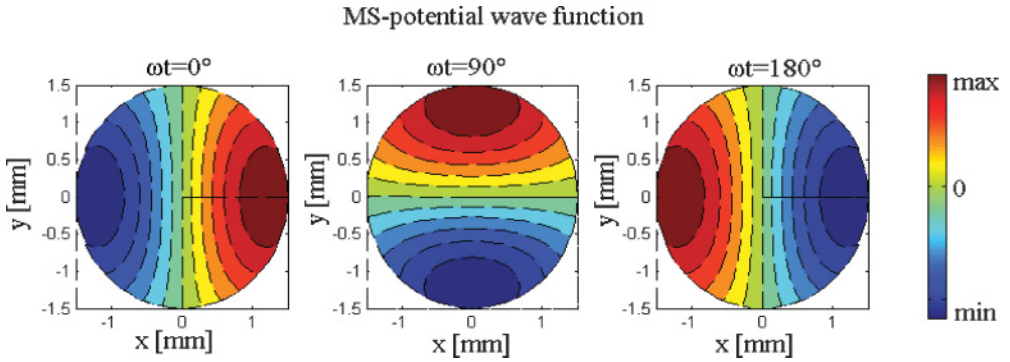

FIG. 1. (Color online) The effective membrane functions $\tilde{\varphi}$ inside a ferrite disk for the first ($n = 1$) MDM at different time phases (arbitrary units).

MDM ferrite disks shown in this article allow a proposition of a special subwavelength microwave metamaterial—the singular-microwave metamaterial. The discovered ability to confine, guide, and manipulate microwaves with topological charges and symmetry-breaking properties on scales that are much smaller than the wavelengths involved appears to be heralding a new field in microwave technology.

Our results presented in this article are mainly based on a numerical analysis. Such a numerical analysis is well justified by our previous analytical and experimental studies of MDM vortices in small ferrite particles [4,5,9,10]. We analyze the field structures for the case of a single ferrite disk and ferrite-disk arrays placed inside a rectangular waveguide. We use a waveguide to properly polarize the external (with respect to a ferrite disk or an array) electromagnetic fields. Studies of other types of external electromagnetic fields are beyond the scope of the present article. One can suppose, however, that since MDM vortices are eigenoscillations in a ferrite disk particle, the observed effects of subwavelength confinement and symmetry breaking will also occur for other types of microwave configurations.

II. LOCALIZED RESONANT STATES OF MICROWAVE ENERGY INSPIRED BY MAGNETIC-DIPOLAR-MODE VORTICES

Symmetry breakings of the localized microwave fields originate from the peculiar symmetry properties of MDM oscillations. The vortex topological structures of MDM oscillations in a normally magnetized quasi-2D ferrite disk become evident from the spectral problem solutions. By assuming a separation of variables for a magnetostatic-potential (MS-potential) wave function in a ferrite disk, a spectral problem in cylindrical coordinates z,r,θ is formulated with respect to membrane MS functions (described by coordinates r,θ) and with amplitudes dependable on the z coordinate. For a dimensionless membrane-MS-potential wave function $\tilde{\varphi}$, the boundary condition of continuity of a radial component of the magnetic flux density on a lateral surface of a ferrite disk of radius $\Re$ is expressed as [2,3]

$$\mu\left(\frac{\partial\tilde{\varphi}}{\partial r}\right)_{r=\Re^-} - \left(\frac{\partial\tilde{\varphi}}{\partial r}\right)_{r=\Re^+} = -i\frac{\mu_a}{\Re}\left(\frac{\partial\tilde{\varphi}}{\partial\theta}\right)_{r=\Re^-}, \quad (1)$$

where μ and μ_a are, respectively, diagonal and off-diagonal components of the permeability tensor $\ddot{\mu}$. The term on the right-hand side (RHS) of Eq. (1) has the off-diagonal component of the permeability tensor μ_a in the first degree. There is also the first-order derivative of function $\tilde{\varphi}$ with respect to the azimuth coordinate. This means that for the MS-potential wave solutions one can distinguish the time direction (given by the direction of the magnetization precession and correlated with a sign of μ_a) and the azimuth rotation direction (given by a sign of $\partial\tilde{\varphi}/\partial\theta$). For a given sign of a parameter μ_a, there are different MS-potential wave functions, $\tilde{\varphi}^{(+)}$ and $\tilde{\varphi}^{(-)}$, corresponding to the positive and negative directions of the phase variations with respect to a given direction of azimuth coordinates, when $0 \leqslant \theta \leqslant 2\pi$.

Suppose that for a given direction of a bias magnetic field, a certain azimuthally running magnetostatic wave acquires a phase Φ_1 after rotation around a disk. For an oppositely directed magnetic field such a phase will be Φ_2. It is evident

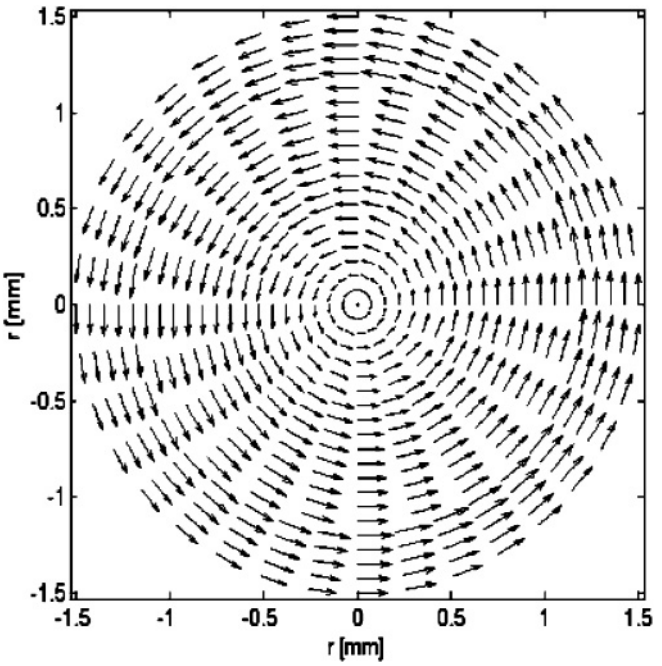

FIG. 2. Analytically derived power-flow-density distribution inside a ferrite disk for the first ($n = 1$) MDM (arbitrary units).

that $|\Phi_1| = |\Phi_2| \equiv \Phi$ and we should have $\Phi_1 + \Phi_2 = 2\pi q$ or $\Phi = q\pi$, where the quantities q are odd integers. This follows from the time-reversal symmetry-breaking effect. A system comes back to its initial state after a full 2π rotation. But this 2π rotation can be reached if both partial rotating processes with phases Φ_1 and Φ_2 are involved. So, minimal $q = 1$ and, generally, q is an odd integer. From the above consideration, one may conclude that for a given direction of a bias magnetic field, a membrane function $\tilde{\varphi}$ behaves as a double-valued function. To make the MS-potential wave functions single-valued and so to make the MDM spectral problem analytically integrable, two approaches have been suggested. These approaches, distinguished by the differential operators and boundary conditions used for solving the spectral problem, give two types of the MDM oscillation spectra in a quasi-2D ferrite disk. Conventionally, these two approaches are named as the *G*- and *L*-modes in the magnetic-dipolar spectra [5,29].

For the *L*-mode spectra, one has the power-flow density vortices inside a ferrite disk. Such vortex behaviors are well justified based on analytical solutions of the MDM spectral problem in a helical coordinate system [29]. With further reduction of the helical-system solutions to the cylindrical-coordinate solutions, one can use separation of variables so that the MS-potential wave function for *L* modes can be written as [4,5,29]

$$\psi_{\nu,n} = C\xi_{\nu,n}(z)\tilde{\varphi}_{\nu,n}(r,\theta), \tag{2}$$

where a dimensionless effective membrane function $\tilde{\varphi}_{\nu,n}(r,\theta)$ is defined by the Bessel-function orders $\nu = 1,2,3,\ldots$ and the numbers of zeros of the Bessel functions corresponding to different radial variations $n = 1,2,3,\ldots$. In Eq. (2), $\xi_{\nu,n}(z)$ is an amplitude factor for a normal-axis coordinate z and C is a dimensional coefficient. Inside a ferrite disk ($r \leqslant \Re$, $-d/2 \leqslant z \leqslant d/2$) the MS-potential wave function is represented as

$$\psi(r,\theta,z,t) = C J_\nu\left(\frac{\beta r}{\sqrt{-\mu}}\right)\left(\cos\beta z + \frac{1}{\sqrt{-\mu}}\sin\beta z\right) e^{-i\nu\theta} e^{i\omega t}, \tag{3}$$

where β is a propagation constant for MS waves along the z axis. Solutions in a form of Eq. (3) show the azimuthally-propagating wave behavior for MS-potential membrane functions. For such an azimuth wave, one has the azimuthal power flow density [4]

$$[p_n(r,z)]_\theta = A\frac{\tilde{\varphi}_n(r)}{8\pi}\omega[\xi_n(z)]^2\left[-\nu\tilde{\varphi}_n(r)\frac{\mu}{r} - \mu_a\frac{\partial\tilde{\varphi}_n(r)}{\partial r}\right], \tag{4}$$

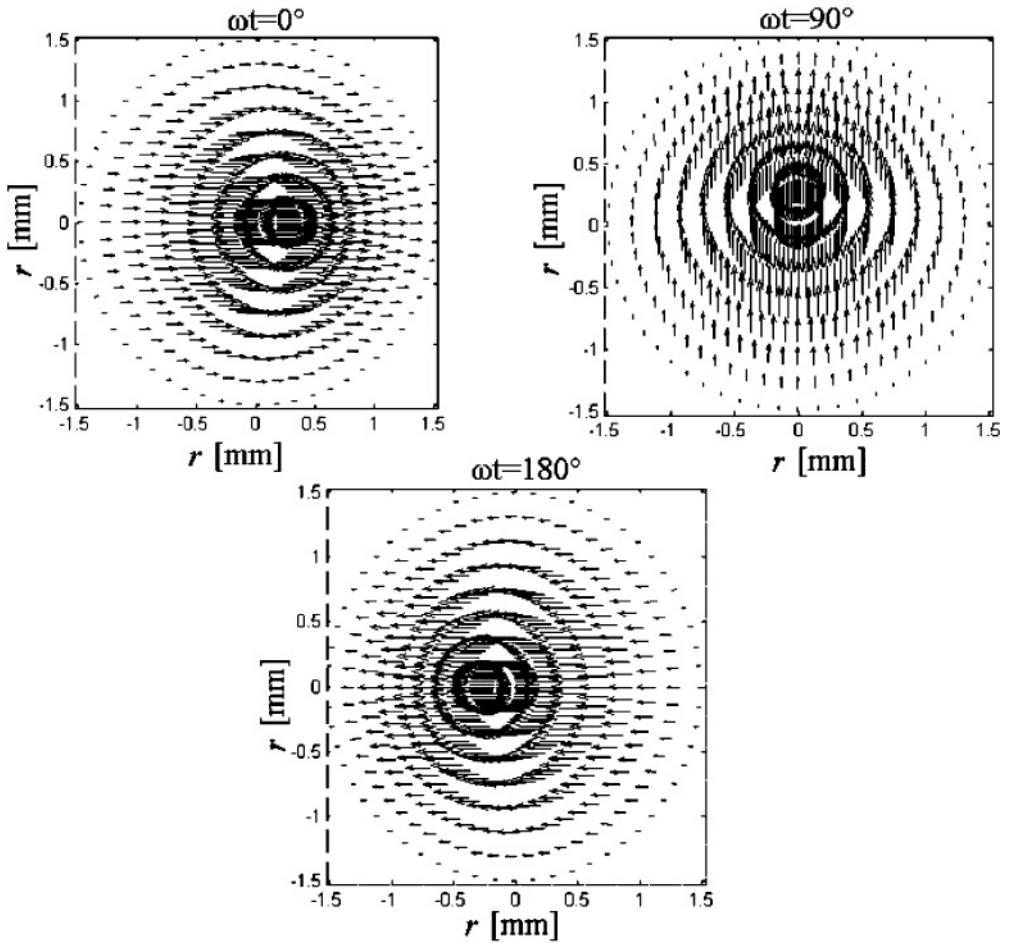

FIG. 3. Analytically derived gallery of magnetization $\vec{m}$ in a ferrite disk at different time phases for the first MDM resonance (arbitrary units).

where A is a dimensional coefficient. This is a nonzero circulation quantity around a circle with circumference $2\pi r$. The amplitude of an MS-potential function is zero at $r = 0$. For a scalar wave function, this presumes the Nye and Berry phase singularity [30]. Circulating quantities $[p_n(r,z)]_\theta$ are the MDM power-flow-density vortices with cores at the disk center. At a vortex center, the amplitude of $(p_n)_\theta$ is equal to zero.

For analytical studies of the spectral properties, we use a lossless ferrite disk with the following material parameters: the saturation magnetization is $4\pi M_s = 1880$ G. The disk diameter is $D = 3$ mm and the disk thickness is $t = 0.05$ mm. The disk is normally magnetized by a bias magnetic field $H_0 = 4900$ Oe. The z dependence of the MS potential in a ferrite disk, defined by the function $\xi(z)$ in Eq. (2), corresponds to the first "thickness" (even) mode, as in our previous studies [2–5]. For a case of $\nu = 1$, the MDM resonant frequencies are $f = 8.548$ GHz for the first MDM ($n = 1$) and $f = 8.667$ GHz for the second MDM ($n = 2$). In our calculations, parameters of the permeability tensor of a ferrite are found for an internal field ($H_i = H_0 - 4\pi M_s$) based on well-known formulas [31]. At the first resonance frequency ($f = 8.548$ GHz) there are $\mu = -26.9869$ and $\mu_a = -28.2965$. At the second resonance frequency ($f = 8.667$ GHz) we have $\mu = -11.2294$ and $\mu_a = -12.5368$. We analyze the power-flow density distribution $\vec{p}$ inside a ferrite disk and also the magnetization $\vec{m}$. For the first ($\nu = 1, n = 1$) MDM, Fig. 1 shows, in arbitrary units, the effective membrane functions $\tilde{\varphi}(r,\theta,t)$ at different time phases and Fig. 2 shows, in arbitrary units, the power-flow density distribution inside a ferrite disk. Figures 3 and 4 show the analytically derived galleries of magnetization $\vec{m}$ in a ferrite disk in arbitrary units for the first ($\nu = 1, n = 1$) and second ($\nu = 1, n = 2$) MDM resonances, respectively, at different time phases. From magnetization pictures it becomes evident that in an analysis of interaction with external electromagnetic fields, an MDM ferrite disk can be modeled as a particle with in-plane rotating magnetic dipoles.

One of important features of the L modes is a very good correspondence between analytical and numerical (based on the HFSS electromagnetic simulation program, produced by the ANSOFT Company) results of the mode characterization [4,5]. This allows the numerical analysis of microwave structures with enclosed MDM ferrite disks. In numerical studies, we used the same disk parameters as for analytical studies and, additionally, took into account small losses in a ferrite sample and dielectric properties of a ferrite. We considered a sample with a linewidth of $\Delta H = 0.8$ Oe and a scalar electric

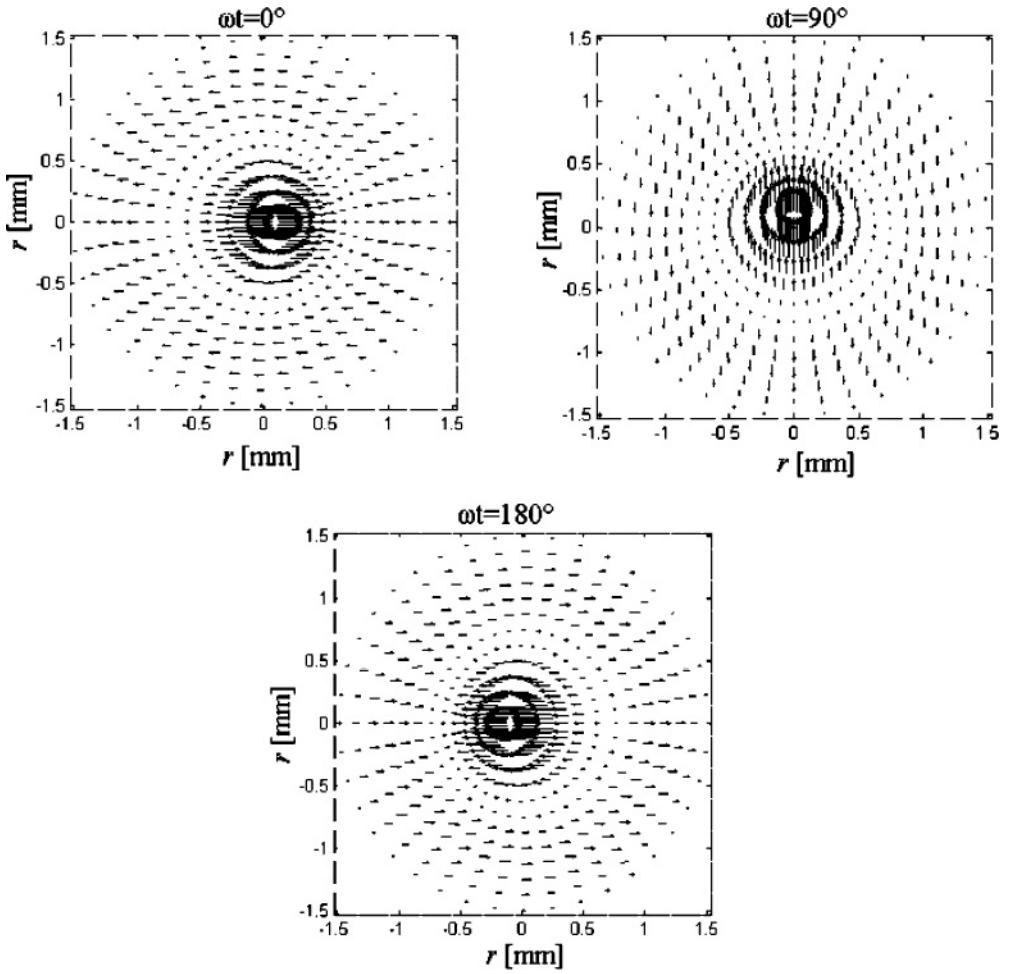

FIG. 4. Analytically derived gallery of magnetization $\vec{m}$ in a ferrite disk at different time phases for the second MDM resonance (arbitrary units).

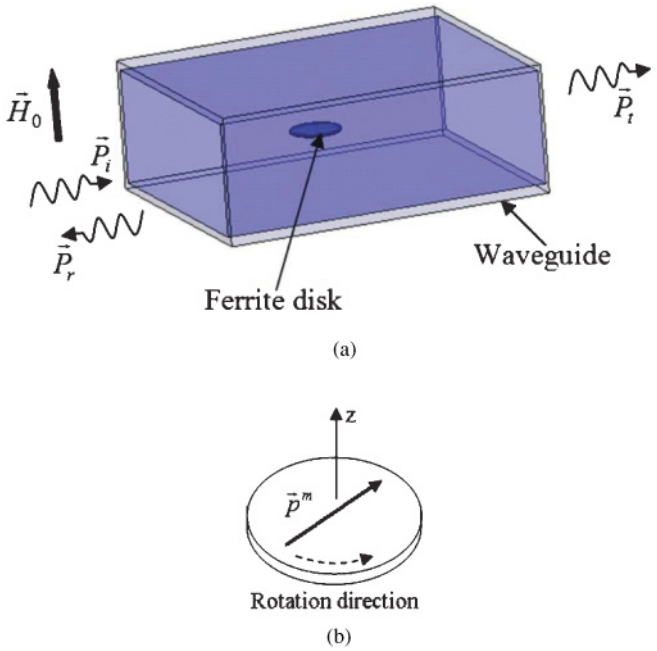

FIG. 5. (Color online) Normally magnetized ferrite disk inside a rectangular waveguide. (a) Geometry of a structure with notations of power flows of incident ($\vec{P}_i$), reflected ($\vec{P}_r$), and transmitted ($\vec{P}_t$) waves. (b) A model of an MDM ferrite disk with an in-plane rotating magnetic dipole $\vec{p}^m$.

permittivity $\varepsilon_r = 15$. Generally, these data correspond to the sample parameters used in microwave experiments [6–10]. A disk is placed inside a TE_{10}-mode rectangular X-band waveguide symmetrically with respect to its walls so that the disk axis is perpendicular to a wide wall of a waveguide. The waveguide walls are made of copper. Figure 5(a) shows geometry of a structure with notations of power flows of incident ($\vec{P}_i$), reflected ($\vec{P}_r$), and transmitted ($\vec{P}_t$) waves. Figure 5(b) represents an MDM ferrite disk as a magnetic dipole $\vec{p}^m$ rotating in a plane perpendicular to the disk normal axis z [5].

For a waveguide with a ferrite disk, a numerical analysis gives a multiresonance frequency characteristic of the reflection (the S_{11} scattering-matrix parameter) and transmission (the S_{21} scattering-matrix parameter) coefficients. These characteristics are represented, respectively, in Figs. 6(a) and 6(b). The resonance peaks are designated in succession by the numbers n. From the absorption ratio $(1 - |S_{11}|^2 - |S_{21}|^2)$, it can be clearly shown that there are absorption peaks at the resonance frequencies. The analytically derived spectral peak positions for the L modes $(\nu = 1; n = 1,2,3)$ [4,5] represented in Fig. 6(c) are in quite good correspondence with the numerically obtained spectral peak positions shown in Figs. 6(a) and 6(b).

To observe the effect of field localization, we analyzed the field structures and the time-average Poynting vector distributions on the xy vacuum plane inside a waveguide situated at 150 mkm above an upper plane of a ferrite disk (Fig. 7). We refer to this vacuum plane as plane A. The Poynting vector pictures on plane A are shown in Figs. 8(a), 8(b), and 8(c). The pictures in Figs. 8(a) and 8(c) are at the frequencies of the first ($f = 8.5225$ GHz) and the second ($f = 8.6511$ GHz) resonances, whereas the picture in Fig. 8(b) is at the frequency between the resonances ($f = 8.5871$ GHz). The corresponding pictures of the in-plane Poynting vector distributions inside a ferrite disk are shown in Figs. 7(d), 7(e), and 7(f). In Figs. 9(a), 9(b), and 9(c) we show, respectively, the magnetic field distributions on plane A at the first resonance frequency $f = 8.5225$ GHz, at nonresonance frequency $f = 8.5871$ GHz and at the second resonance frequency $f = 8.6511$ GHz. To watch the dynamics, the fields are represented for two phases: $\omega t = 0^\circ$ and $\omega t = 90^\circ$. As a very important property of the observed pictures of the magnetic field distributions, there is an evident rotating-magnetic-dipole behavior at resonance frequencies [see Figs. 9(a) and 9(c)].

It is obvious that, at the MDM resonant frequencies, there are vortices of the Poynting vector distributions with strong subwavelength confinement of the electromagnetic energy. No such confinement is observed at nonresonance frequencies. The fact that the MDM vortices are the origins of the 3D electromagnetic (EM) field confinement is evident both in the xy plane and in the normal axis z direction. Regarding confinement in the z direction, one can see from Fig. 8 that at the resonance frequency, the power-flow density on plane A is about three orders of magnitude less than the Poynting vector quantity inside a ferrite disk. It is evident also that, at MDM resonances, there are strong field concentrations and symmetry violations. No field enhancement and no symmetry violation occur at nonresonance frequencies. Resonant-state localization of microwave energy inspired by MDM vortices can be revealed from an analysis of the energy densities of the fields in a hollow waveguide and inside a ferrite disk. We define the energy density as

$$w = S/v_g, \tag{5}$$

where S is the power flow density and v_g is a group velocity. A group velocity v_g^w of EM waves in a hollow waveguide is expressed as [32]

$$v_g^w = c\sqrt{1 - (f_c/f)^2}, \tag{6}$$

where c is the speed of light and f_c is the cutoff frequency of a TE mode. For a TE_{10}-mode rectangular X-band waveguide, one has $f_c = 6.562$ GHz. This gives for the first-resonance frequency ($f = 8.5225$ GHz) $v_g^w = 0.638c$ and for the second-resonance frequency ($f = 8.6511$ GHz) $v_g^w = 0.652c$. Analytical solutions for a group velocity v_g^m of azimuthally propagating modes inside a ferrite disk should be obtained based on an analysis of the MDM spectral problem in a helical coordinate system [29]. Such an analytical study of group velocities in the MDM spectrum is beyond the scope of the present article. Magnetic-dipolar modes are strongly dispersive waves [31] and so the group velocity v_g^m should be much less than the phase velocity v_{ph}^m of azimuthally-propagating MDMs. However, we will use here a phase velocity v_{ph}^m as an upper limit of a group velocity v_g^m. We will estimate a phase velocity as a linear velocity of a circular motion of a "magnetic charge" of a rotating magnetic dipole. Thus, we can write

$$\left(v_g^m\right)_{\max} = v_{ph}^m = 2\pi \Re f. \tag{7}$$

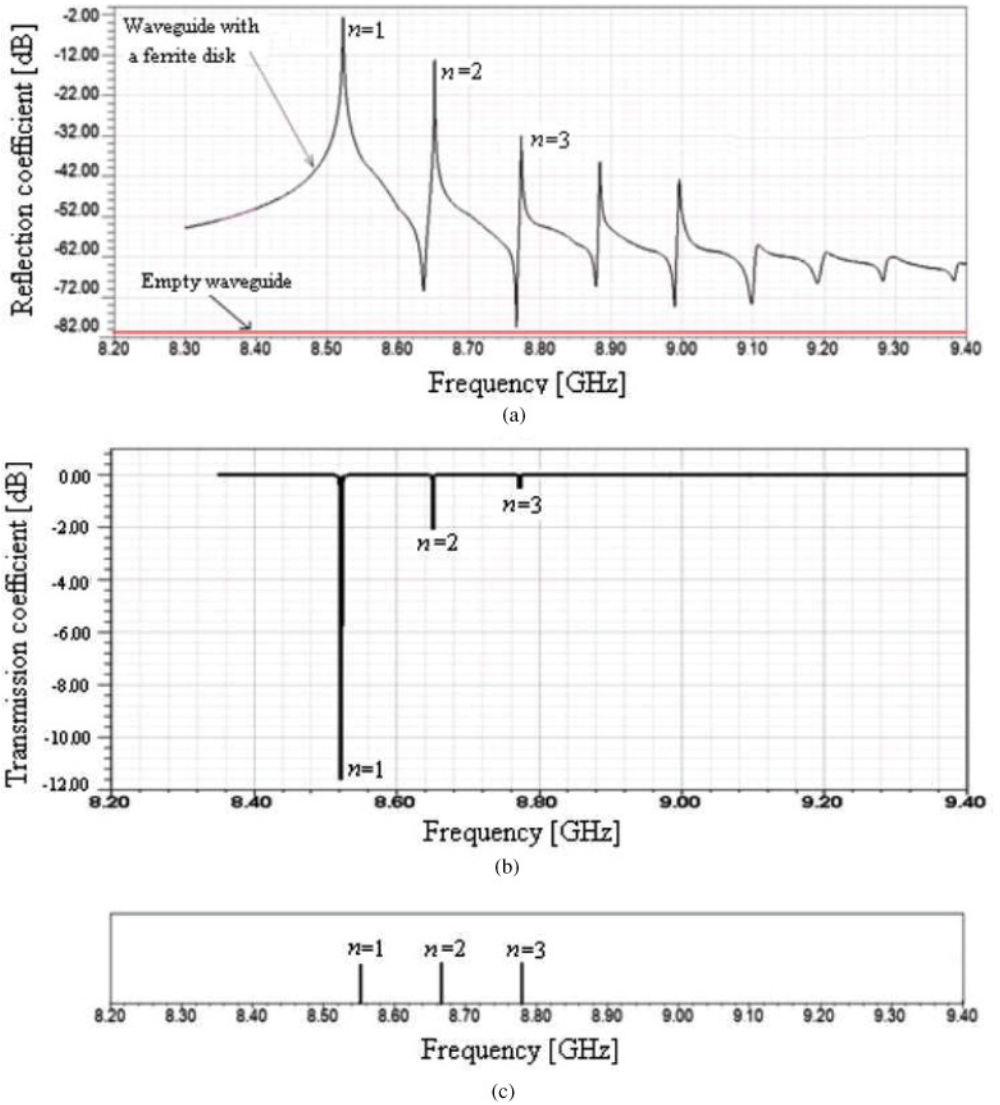

FIG. 6. (Color online) MDM resonances of a quasi-2D ferrite disk. (a) The numerically obtained multiresonance frequency characteristic of the reflection coefficient. (b) The numerically obtained multiresonance frequency characteristic of the transmission coefficient. (c) The analytically derived spectral peak positions for the first three ($\nu = 1; n = 1,2,3$) MDM resonances.

At the disk diameter $2\Re = 3$ mm, we have for the first and second resonance frequencies, respectively: $(v_g^m)_{\max} = v_{ph}^m = 0.267c$ and $(v_g^m)_{\max} = v_{ph}^m = 0.272c$. There is an approximate relationship between the waveguide and the ferrite-disk group velocities for both resonance frequencies:

$$v_g^w \big/ \left(v_g^m\right)_{\max} \approx 2.4. \tag{8}$$

From pictures of the power-flow-density distributions (Fig. 8) it follows that at resonance frequencies, the power-flow density in a hollow waveguide is at least three orders of magnitude less than the power-flow density inside a ferrite disk. Taking into account Eqs. (5) and (8), very strong localization of microwave energy becomes evident [more than three orders of magnitudes even using the condition $(v_g^m)_{\max} = v_{ph}^m$], inspired by magnetic-dipolar-mode vortices. It is worth noting that there are discrete states of energy: no effect of the energy localization takes place at nonresonance frequencies.

Every resonant state is characterized by a strong pronounced eigenfunction pattern with a topologically distinct vortex structure. The observed Poynting vector distributions are spiral waves emitted by a scatterer—the MDM ferrite disk. Such waves appear due to interaction of the MDM vortex core with the TE-mode wave train. The vortex core, with a

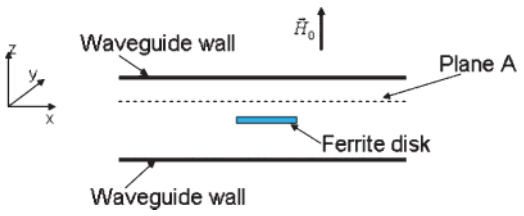

FIG. 7. (Color online) The *xy* vacuum plane inside a waveguide situated at the distance of 150 mkm above an upper plane of a ferrite disk. This vacuum plane is conventionally called plane A.

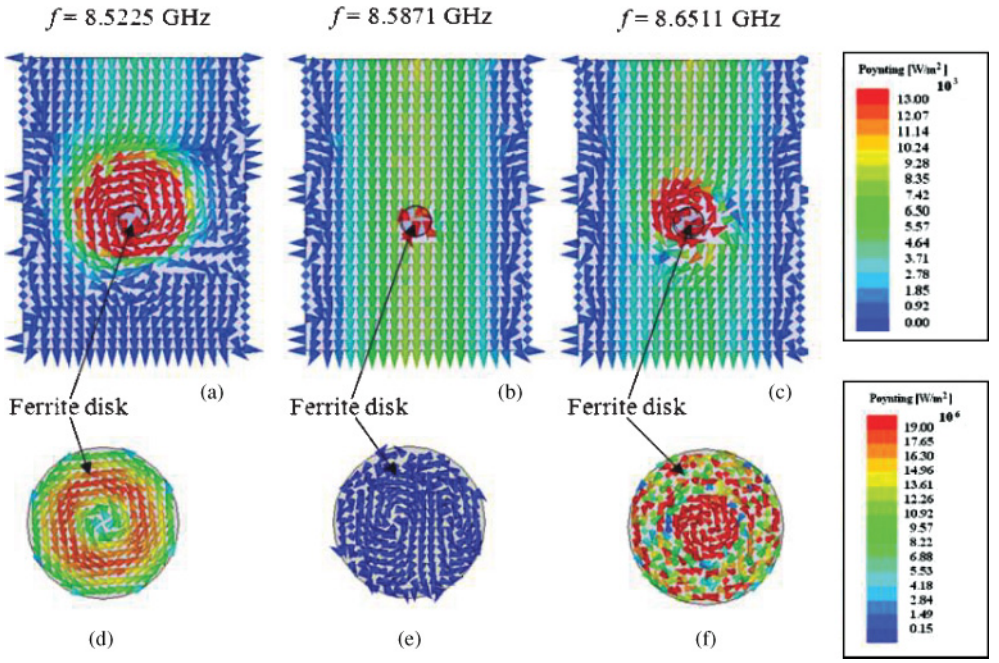

FIG. 8. (Color online) Field confinement originating from the MDM vortices in a ferrite disk. (a) The Poynting vector distributions for the field on plane A at the frequency ($f = 8.5225$ GHz) of the first resonance. (b) The same at the frequency ($f = 8.5871$ GHz) between the resonances. (c) The same at the frequency ($f = 8.6511$ GHz) of the second resonance. (d) The Poynting vector distributions inside a ferrite disk at the frequency of the first resonance. (e) The same at the frequency between resonances. (f) The same at the frequency of the second resonance.

diameter equal approximately to the ferrite disk diameter, is impenetrable for the TE_{10} waveguide mode. It is a singular region (a topological defect) for the TE_{10} waveguide mode. Unique topological properties of the scattered EM spiral waves can be revealed based on an analysis of the structure of the electric fields. Incline views of the electric field distributions on plane A for the first resonance frequency ($f = 8.5225$ GHz) at two phases ($\omega t = 0^\circ$ and $\omega t = 90^\circ$) are shown in Fig. 10. One can see that the electric field preserves its TE polarization (with respect to the z direction), with the exception of the disk region. At the core region, the electric field has dominating in-plane (xy plane) components. It is evident (compare the magnetic and electric field distributions in Figs. 9 and 10, respectively) that in the region of a disk center, the in-plane magnetic and electric fields are mutually parallel and so the Poynting vector in the vortex core is equal to zero.

For TE polarized (with respect to the z direction) electromagnetic waves, the singular features of the complex electric field component $E_z(x,y)$ can be related to those that will subsequently appear in the associated 2D time-averaged real-valued Poynting vector field $\vec{S}(x,y)$. The transport of electromagnetic energy through the waveguide is described by the Poynting vector

$$\vec{S} = \frac{c}{4\pi}[\mathrm{Re}(\vec{E}_c e^{i\omega t}) \times \mathrm{Re}(\vec{H}_c e^{i\omega t})], \tag{9}$$

where $\vec{E}_c$ and $\vec{H}_c$ are complex amplitudes of the field vectors. From the Maxwell equation in a vacuum one has

$$\mathrm{Re}(\vec{H}_c e^{i\omega t}) = \frac{c}{\omega}\mathrm{Im}\,[\nabla \times (\vec{E}_c e^{i\omega t})]. \tag{10}$$

Thus, Eq. (9) can be rewritten as

$$\vec{S} = \frac{c^2}{4\pi\omega}\{\mathrm{Re}(\vec{E}_c e^{i\omega t}) \times [\nabla \times \mathrm{Im}\,(\vec{E}_c e^{i\omega t})]\}. \tag{11}$$

We take advantage now of the following vector relation for two arbitrary vectors $\vec{a}$ and $\vec{b}$. If one supposes that these vectors have only one component (let it will be the z component), one evidently has $\vec{a} \times (\nabla \times \vec{b}) = a_z \vec{\nabla}_\perp b_z$, where $\nabla_\perp$ is the differential operator with respect to the x and y coordinates. When electromagnetic fields are invariant with respect to the z direction, it is possible to represent a time-averaged part of the Poynting vector as

$$\langle \vec{S} \rangle = \frac{c^2}{8\pi\omega}\mathrm{Im}\,(E_z^* \vec{\nabla}_\perp E_z), \tag{12}$$

where E_z is a complex vector of the z component of the electric field: $E_z \equiv (E_c)_z e^{i\omega t}$. The fact that, for electromagnetic fields invariant with respect to a certain coordinate, a time-averaged part of the Poynting vector can be approximated by a scalar wave function, makes it possible to analyze the vortex phenomena. For a TE-polarized field, we can write

$$E_z(x,z) \equiv \Theta(x,y) = \rho(x,y) e^{i\chi(x,y)}, \tag{13}$$

where ρ is an amplitude and χ is a phase of a scalar wave function Θ. One can rewrite Eq. (12) as

$$\langle \vec{S} \rangle = \rho(x,y)^2 \nabla_\perp \chi(x,y). \tag{14}$$

This representation of the Poynting vector in a quasi-2D system allows one to clearly define a phase singularity as a point (x,y) where the amplitude ρ is zero and hence the phase χ

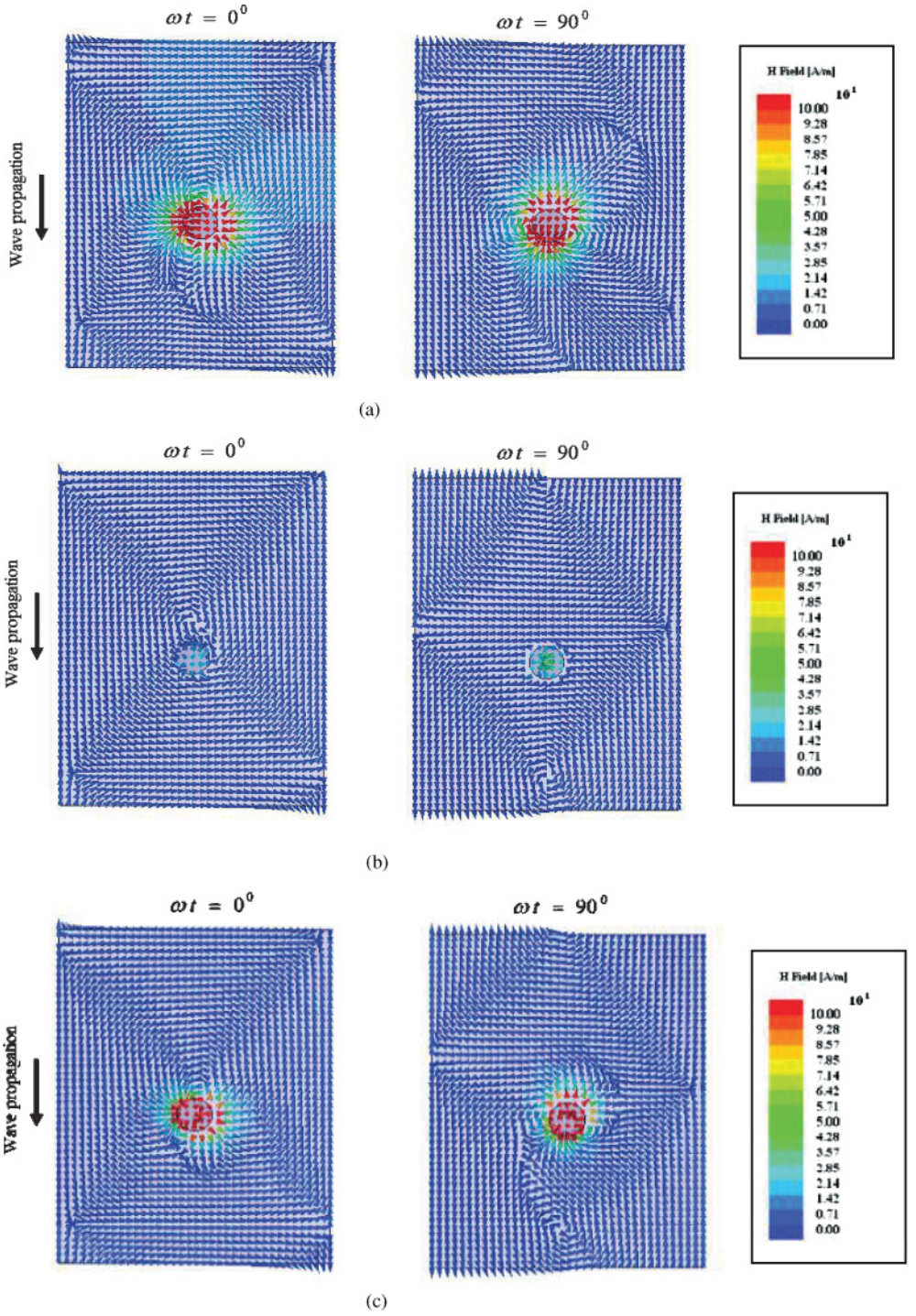

FIG. 9. (Color online) Evidence for correlation between strong field concentrations and symmetry violations at MDM resonances. (a) The magnetic field distributions on plane A at the frequency ($f = 8.5225$ GHz) of the first resonance for the two phases $\omega t = 0^\circ$ and $\omega t = 90^\circ$. (b) The same at the frequency ($f = 8.5871$ GHz) between the resonances. (c) The same at the frequency ($f = 8.6511$ GHz) of the second resonance.

is undefined. Such singular points of $E_z(x,z)$ correspond to vortices of the power flow $\langle \vec{S} \rangle$, around which the power flow circulates. A center is referred to as a (positive or negative) topological charge. Since such a center occurs in free space without energy absorption, it is evident that $\nabla_\perp \cdot \langle \vec{S} \rangle = 0$. When we take a certain circle C of radius R surrounding a vortex core ($R > \Re$), a topological charge is defined as a circulation around C:

$$\gamma = \frac{1}{2\pi R} \oint_C \nabla_\perp \chi \cdot d\vec{C} = \frac{1}{2\pi} \int_0^{2\pi} \nabla_\perp \chi \cdot d\vec{\theta}, \qquad (15)$$

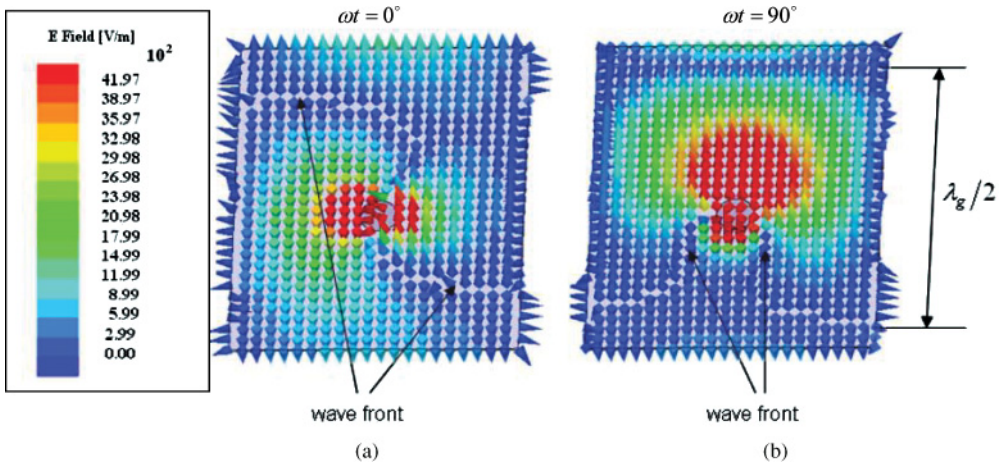

FIG. 10. (Color online) Electric field distributions on plane A at the frequency ($f = 8.5225$ GHz) of the first resonance for the two phases $\omega t = 0^\circ$ and $\omega t = 90^\circ$ (inclined views). The guide wavelength is λ_g.

where we used $d\vec{C} = Rd\vec{\theta}$, with θ being an azimuth coordinate for rotations along a circle C.

Scattering of the EM fields from the MDM-vortex particle is purely topological. In Fig. 10, one can see a strong distortion of the wave front in a region of an MDM vortex. For an incident microwave flow of a TE mode, a rotating-magnetic-dipole ferrite particle appears as a small region of a moving (rotating) medium. The flow velocity of such a rotating medium can be estimated as v_g^m. As we discussed above, the group velocity of azimuthally-propagating modes inside a ferrite disk should be much smaller than the group velocity of EM waves in a hollow waveguide: $v_g^m \ll v_g^w$, which means that for an incident microwave flow of a TE mode, an MDM ferrite disk is represented as a slowly moving medium. Berry *et al.* [33] showed an analogy between waves in the presence of a vector potential (the Aharonov-Bohm effect [34]) and waves in a slowly moving (rotating) medium. In the case of waves in a moving medium, the analog of the quantum flux parameter (which gives a geometric phase in the Aharonov-Bohm effect) α is defined via a circular integration of the flow velocity in a medium [33]. In Refs. [33,35], the regions of contrast phases of the water waves in a tank were experimentally studied on a subject of influence of a filamentary vortex. The experiments verified the analogy between such a classical mechanics system and the quantum mechanical Aharonov-Bohm effect. It was pointed out also [35] that the most striking difference between the quantum mechanical case and the case of water waves in a filamentary vortex is nonsymmetry of the classical scattered waves due to the vortex core rotation. Our studies of the interaction of a TE mode with MDM vortices show effects similar to those shown in the water experiments [33,35]. We also observe nonsymmetry for electromagnetic-field-scattered MDM vortices. From Fig. 10, it follows that an electric field is a nonsymmetric function: $E_z(\theta^{(+)}) \neq E_z(\theta^{(-)})$, where $\theta^{(\pm)}$ is an azimuth coordinate for counterclockwise (+) and clockwise (–) rotations along a circle C. The power-flow-density vortices in Figs. 8(a) and 8(c) are similar to water spiral waves scattered from a filamentary vortex in Ref. [35]. Spiral waves appear when the rotation symmetry at the vortex core is broken and takes place due to a phase shift in a dislocated plane wave. A geometrical phase can be calculated from the dislocation structure of the waves, which depends, in turn, on the flux parameter α [33].

In this section of the article, we showed that the observed bound states in a microwave waveguide inspired by magnetic-dipolar-mode vortices are characterized by strong energy localization in the vicinity of the ferrite particle. We gave a preliminary analysis of topological properties of the localized resonant states of EM energy. Unique symmetry violation effects for microwave fields due to MDM vortex particles need a more detailed analysis. This should be a subject for further considerations.

III. MDM-VORTEX-PARTICLE ARRAYS: PROPOSAL FOR MICROWAVE SUBWAVELENGTH METAMATERIALS

The MDM ferrite disks have very peculiar near-field-interaction behavior. The fact that every disk acts as a rotating magnetic dipole and has a vortex behavior makes

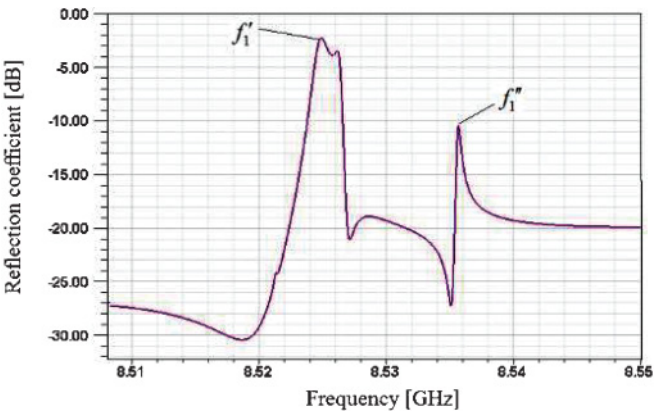

FIG. 11. (Color online) Splittings of the MDM resonance peaks in a chain of quasi-magnetostatically interacting ferrite disks. In an analysis of a disk chain, two resonance frequencies $f_1' = 8.5248$ GHz and $f_1'' = 8.5356$ GHz are chosen.

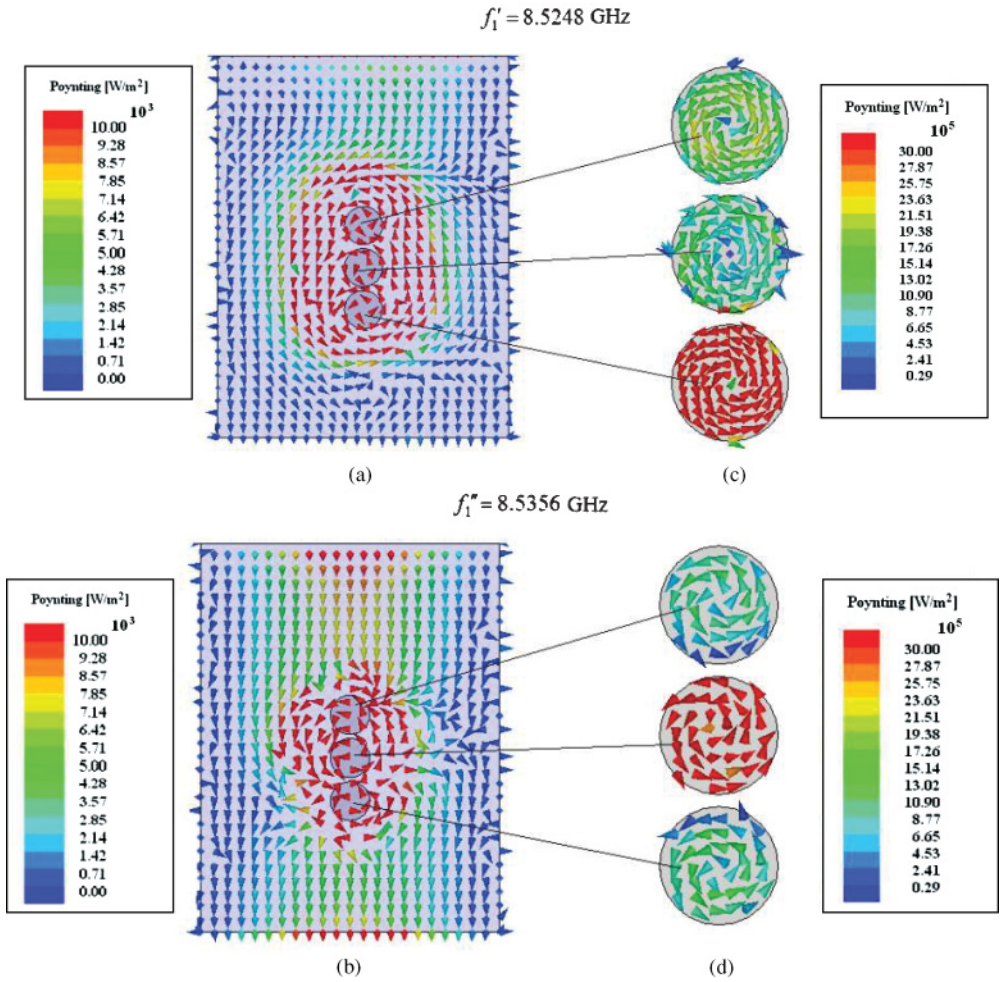

FIG. 12. (Color online) The field confinement originating from the MDM vortices in a chain of interacting ferrite disks. (a) The Poynting vector distribution on plane A at resonance frequency $f_1' = 8.5248$ GHz. (b) The same at resonance frequency $f_1'' = 8.5356$ GHz. (c) The pictures of the Poynting vector distributions inside every ferrite disk in a chain at resonance frequency $f_1' = 8.5248$ GHz. (d) The same at resonance frequency $f_1'' = 8.5356$ GHz.

the problem solution nontrivial. The *G*-mode and *L*-mode approaches used in an analysis of the magnetic-dipolar spectra [5,29] presume different mechanisms in describing MDM-particle interactions. Recently, an analytical model for *G*-mode interacting MDM-vortex particles has been developed [36]. It was shown that an interaction between such particles differs from purely magnetostatic interactions between two magnetic dipoles. There is an essential role of the electric fields in such interactions. In the present article, we study numerically (based on the HFSS program) the near-field structures of interacting *L*-mode ferrite disks with power-flow-density vortices. One can suppose that, in such structures, interactions between adjacent ferrite-disk particles will set up coupled MDM-EM modes with coherent energy transport along the particle arrays. The vortex behaviors of the MDM ferrite particles should presume the microwave field properties very different from the point-dipole-array fields in optical-frequency structures with plasmonic oscillations [21,22].

As an initial stage of an analysis, we consider a chain of ferrite magnetic-dipolar-vortex particles with the evanescent-tail coupling between adjacent MDM resonators. In our numerical study, an in-plane chain of three quasi-2D normally magnetized ferrite disks is placed inside a TE_{10}-mode rectangular waveguide symmetrically with respect to its walls. The chain is stretched along a waveguide axis. The disk diameters are 3 mm and distances between the disk centers are 3.2 mm. By virtue of the near-field interactions between the disks, there are splittings of MDM resonance peaks. Figure 11 shows such splitting in the reflection coefficient characteristic of the first resonance peak [see Fig. 6(a)]. For our analysis of a disk chain, we will choose two resonance frequencies designated in Fig. 11 as f_1' and f_1''. In Figs. 12(a) and 12(b), we show the Poynting vector distributions on plane A at resonance frequencies $f_1' = 8.5248$ GHz and $f_1'' = 8.5356$ GHz, respectively. The pictures of the Poynting vector distributions inside every ferrite disk in Figs. 12(c) and 12(d) show that the observed effect of subwavelength confinement of the electromagnetic fields by a disk chain is due to the MDM-resonance vortex behaviors of the particles. For a ferrite-disk chain, the magnetic field distributions on plane A at resonance frequencies $f_1' = 8.5248$ GHz and $f_1'' = 8.5356$ GHz and for two phases $\omega t = 0^\circ$ and $\omega t = 90^\circ$ are shown in Fig. 13. There

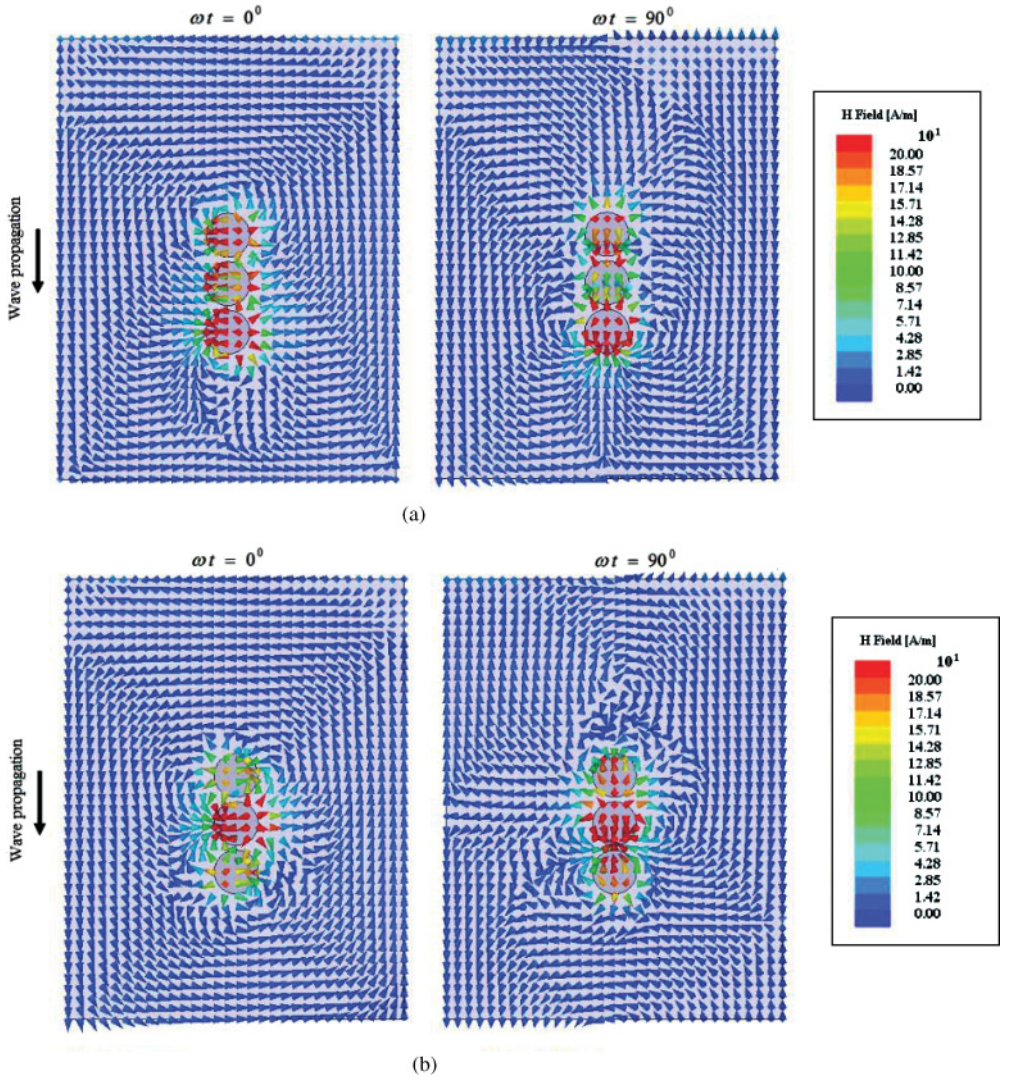

FIG. 13. (Color online) Magnetic field distribution vortices in a chain of interacting ferrite disks. (a) The magnetic field distributions on plane A at the resonance frequency $f_1' = 8.5248$ GHz for the two phases $\omega t = 0^\circ$ and $\omega t = 90^\circ$. (b) The same at the resonance frequency $f_1'' = 8.5356$ GHz. There is evidence of field enhancement in a region near a disk chain. One can clearly observe the rotating-magnetic-dipole behavior of every ferrite disk in the chain. At resonant frequency f_1', all disks oscillate in phase. At resonant frequency f_1'', there are in-phase oscillations for two extreme disks, while an interior disk oscillates in an opposite phase.

is evident field enhancement in a region near a disk chain. One can clearly observe the rotating-magnetic-dipole behavior of every ferrite disk in the chain. At two resonance frequencies, there are different relationships between magnetic field phases in ferrite disks. At resonant frequency f_1', all disks oscillate in phase [see Fig. 13(a)]. At resonant frequency f_1'', there are in-phase oscillations for two extreme disks, while an interior disk oscillates in an opposite phase [see Fig. 13(b)]. Here, we considered a terminated chain of quasi-2D ferrite disks. There are standing magnetic-dipolar waves along such a chain. One can expect that for an infinite structure, an interaction between a chain of magnetic-dipole particles and the electromagnetic field will give the propagation behavior of magnetic-dipolar waves along the chain. At the same time, in the directions perpendicular to the chain, the fields will exponentially decay.

Very unique properties of the MDM-vortex-particle arrays become apparent when a structure has a center of symmetry. Figures 14 and 15 show, respectively, the frequency characteristics of the reflection and transmission coefficients, while Figs. 16 and 17 show, respectively, the power-flow-density distribution and the magnetic-field picture for a structure of an in-plane nine-particle array with a center of symmetry. The transmission and reflection frequency characteristics in Figs. 14 and 15 have very rich and non-regular multiresonance spectra. One can observe a certain frequency band behavior. A peculiar property of a structure with a center of symmetry is a rotating wave running around the entire array. The power-flow-density distribution on plane A shown in Fig. 16 for frequency $f = 8.5225$ GHz gives evidence for the Poynting vector rotations in the regions above every ferrite disk with the exception of the region above a central disk. There is a resulting

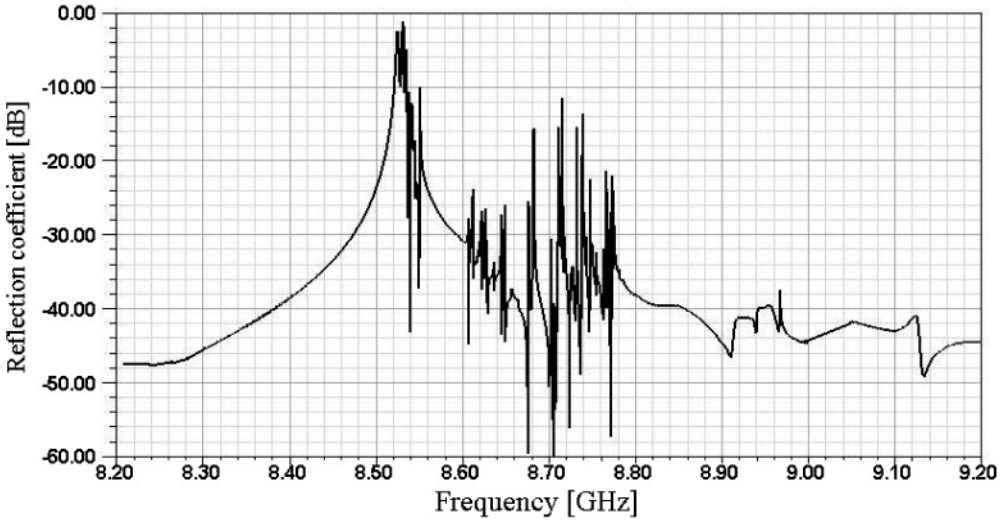

(a)

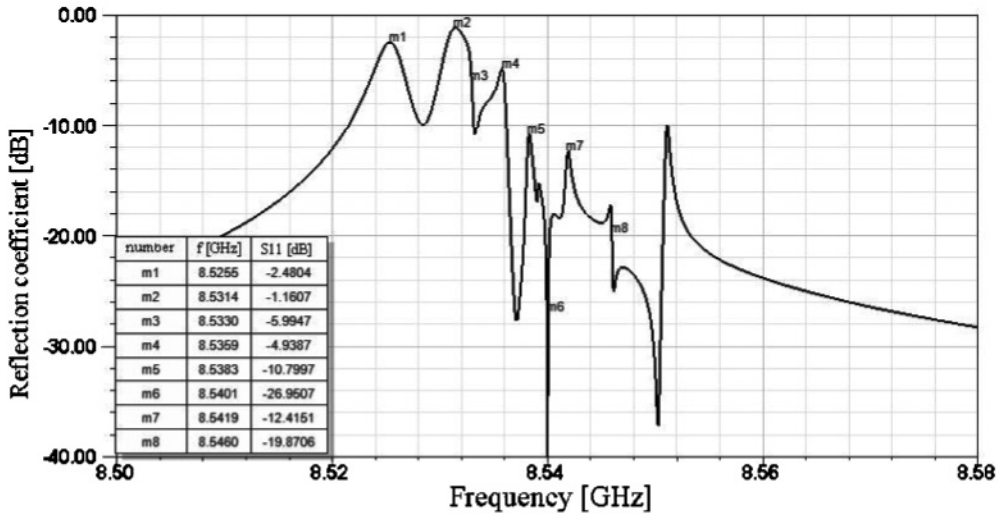

(b)

FIG. 14. The frequency characteristics of the reflection coefficient for MDM resonances in a nine-disk array of quasi-2D ferrite disks. (a) General picture and (b) a zoomed picture of splittings of the MDM resonance peaks.

counterclockwise rotation of the Poynting vector around the entire array. For the same frequency of $f = 8.5225$ GHz, the magnetic-field picture on plane A gives evidence for magnetic dipoles rotating around centers of the disks and around a center of the structure (see Fig. 17). These magnetic dipoles are conventionally shown by black arrows in Fig. 17. Every magnetic dipole has the counterclockwise rotation in time. For a certain phase of time, a circulation around the entire array shows a dynamics process in correlation with cyclic geometrical phase evolution of the disk-magnetic-dipole moments. For 2π circulation, the magnetic-dipole vector accomplishes the 2π geometric-phase rotation. It is worth noting that the direction of the geometric-phase rotation is opposite to the direction of circulation. The results give evidence for a unique property of circulation of topological excitations around a center of symmetry of an array. One of the important features of an array structure with a center of symmetry is a very strong field localization in comparison with other MDM-vortex structures [compare, for example, Figs. 8(a) and 16].

Topological pointlike solutions with coreless 3D textures—the Skyrmions—are well known in nuclear and elementary particle physics [37]. Stable pointlike Skyrmions can be observed in a trapped Bose-Einstein condensate [38]. Based on an array of interacting MDM ferrite disks, one can realize subwavelength microwave structures (microwave subwavelength metamaterials) with channeling of Skyrmion-like topological excitations (channeling of EM power-flow vortices). Special attention should be paid for novel axially symmetric metamaterial structures with rotational channeling of Skyrmion-like topological excitations. The unique symmetry properties of the system of interacting MDM ferrite disks shown in this article

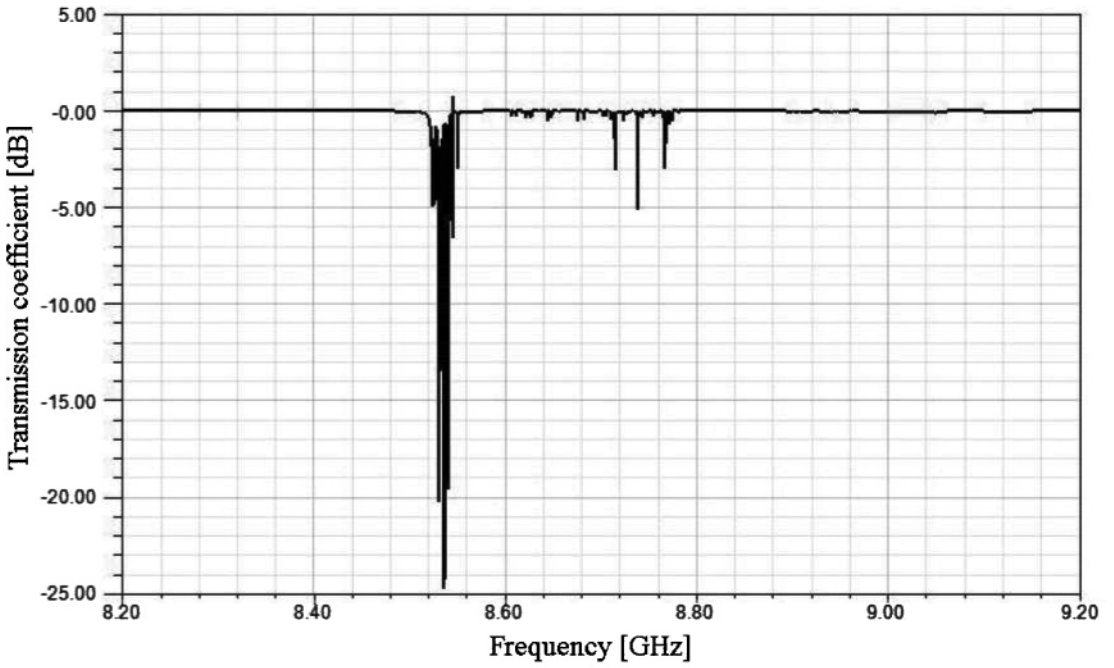

(a)

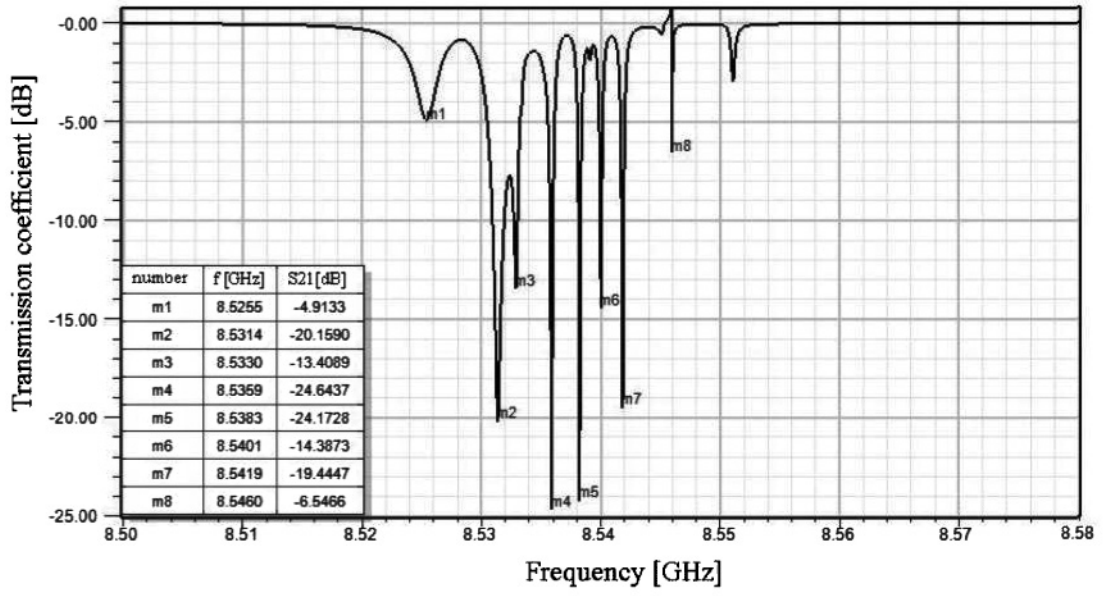

number	f [GHz]	S21 [dB]
m1	8.5255	-4.9133
m2	8.5314	-20.1590
m3	8.5330	-13.4089
m4	8.5359	-24.6437
m5	8.5383	-24.1728
m6	8.5401	-14.3873
m7	8.5419	-19.4447
m8	8.5460	-6.5466

(b)

FIG. 15. Frequency characteristics of the transmission coefficient for MDM resonances in a nine-disk array of quasi-2D ferrite disks. (a) General picture and (b) a zoomed picture of splittings of the MDM resonance peaks.

lead to the proposition of a special subwavelength microwave metamaterial—the singular-microwaves metamaterial.

IV. CONCLUSION AND DISCUSSIONS

In the MDM resonances, precessing electron spins interact collectively with the microwave fields. Due to this effect, one can observe strong localization of EM energy at the MDM resonance frequencies. At the MDM resonance states, the MDM vortices act as traps, providing purely subwavelength confinement of the EM field. The fields outside a ferrite disk are evanescent in nature; they decay exponentially with distance from the ferrite surface.

Based on the analysis made in this article, some future directions and challenges can be suggested for discussion:

In optics, it was recently shown that an array of evanescent-tail-coupling nanoparticle plasmonic resonators is an effective waveguide structure with low loss [22]. This is the demonstration of non-diffraction-limited guiding of electromagnetic energy over micron and submicron distances. Due to the

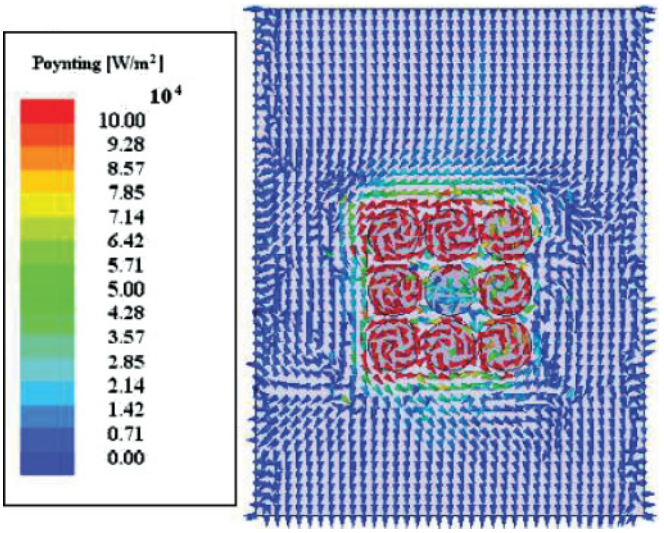

FIG. 16. (Color online) The power-flow-density distribution on plane A for a structure of an in-plane nine-particle array with a center of symmetry.

heightened local fields surrounding plasmonic-resonator guiding structures, such optical devices have potential applications not only in photonics and telecommunications but also in localized biological sensing of molecules. Similarly to a system of coupled plasmonic resonators in optics, we have here effective non-diffraction-limited microwave waveguides. One can suppose that an array of MDM-disk resonators coupled by quasi-magnetostatic evanescent tails will be an effective microwave waveguide structure with low loss. Symmetry breakings of near fields in such structures will allow localized sensing of chiral biological and chemical objects in microwaves.

The interaction of microwave fields with an MDM ferrite disk results in Poynting vector singularities. The power-flow-density vortices in arrays of ferrite disks are well-localized topological excitations that do not perturb the field at large distances from the particles. Based on an array of interacting MDM ferrite disks, one can assume the realization of subwavelength microwave-photonics crystal structures with channeling of Skyrmion-like topological excitations (channeling of EM power-flow vortices).

Interactions between microwave electromagnetic fields and quasi-2D ferrite disks with MDM oscillations can be limited not only to the electromagnetic wave propagation in structures with subwavelength dimensions. Dipolar-mode magnonics of ferrite particles can also help to generate and manipulate microwave electromagnetic radiation. As a cogent argument, one can presuppose that special microwave structures with rotating magnetic fields can be realized so that the phase of a rotating magnetic dipole of an MDM ferrite disk, enclosed in such a microwave structure, will be opposite to the phase of a microwave magnetic field. In this case, the rotational energy of a magnetic dipole of the ferrite-disk particle can be used to create an effective microwave subwavelength antenna. The microwave radiation in such a subwavelength antenna will appear as a result of collective interaction of precessing electron spins in a high-Q-factor MDM ferrite resonator with a magnetic field of a microwave structure.

It is worth noting that the effect of the field localization, observed from our numerical studies, gives evidence for very large field intensity in a ferrite sample. This, certainly, may presume the possibility of nonlinear effects in a ferrite. The question of such nonlinear effects in a ferrite sample is beyond of the scope the present study. This problem should be one of the most important subjects in future studies of the field localization effects due to the MDM ferrite particles.

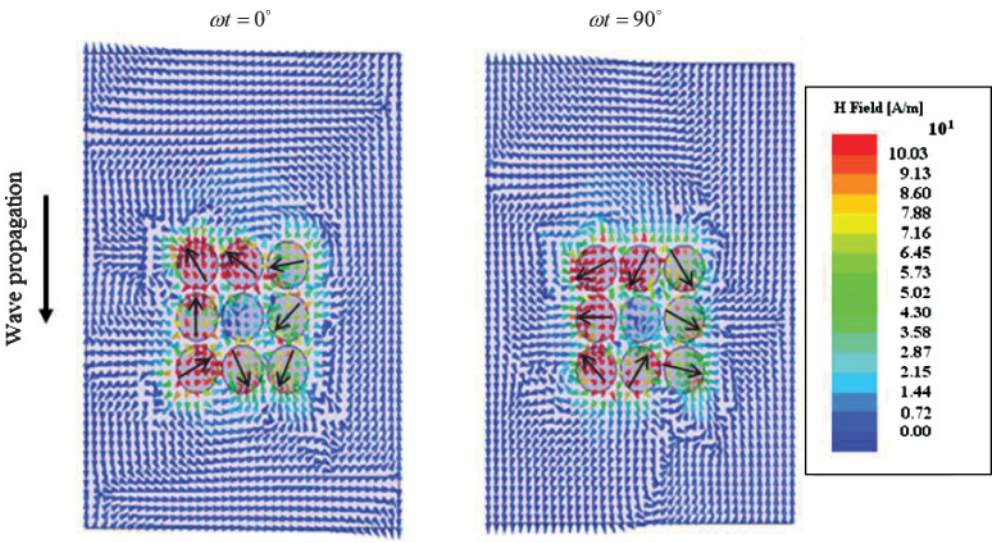

FIG. 17. (Color online) The magnetic-field picture on plane A for a structure of an in-plane nine-particle array with a center of symmetry. Magnetic dipoles of the disks are shown conventionally by black arrows.

[1] E. O. Kamenetskii, Phys. Rev. E **63**, 066612 (2001).
[2] E. O. Kamenetskii, M. Sigalov, and R. Shavit, J. Phys. Condens. Matter **17**, 2211 (2005).
[3] E. O. Kamenetskii, J. Phys. A **40**, 6539 (2007).
[4] M. Sigalov, E. O. Kamenetskii, and R. Shavit, J. Phys. Condens. Matter **21**, 016003 (2009).
[5] E. O. Kamenetskii, M. Sigalov, and R. Shavit, J. Appl. Phys. **105**, 013537 (2009).
[6] J. F. Dillon Jr., J. Appl. Phys. **31**, 1605 (1960).
[7] T. Yukawa and K. Abe, J. Appl. Phys. **45**, 3146 (1974).
[8] E. O. Kamenetskii, A. K. Saha, and I. Awai, Phys. Lett. A **332**, 303 (2004).
[9] M. Sigalov, E. O. Kamenetskii, and R. Shavit, Appl. Phys. B **93**, 339 (2008).
[10] M. Sigalov, E. O. Kamenetskii, and R. Shavit, J. Appl. Phys. **104**, 053901 (2008).
[11] W. S. Ishak and K. Chang, IEEE Trans. Microwave Theory Tech. **34**, 1383 (1986).
[12] M. S. Soskin and M. V. Vasnetsov, *Progress in Optics*, edited by E. Wolf (North-Holland, Amsterdam, 2001), Vol. 42, p. 219.
[13] H. F. Schouten, T. D. Visser, and D. Lenstra, J. Opt. B **6**, S404 (2004).
[14] M. Perez-Molina, L. Carretero, P. Acebal, and S. Blaya, J. Opt. Soc. Am. A **25**, 2865 (2008).
[15] G. D'Aguanno, N. Mattiucci, M. Bloemer, and A. Desyatnikov, Phys. Rev. A **77**, 043825 (2008).
[16] W. L. Barnes, A. Dereux, and T. W. Ebbesen, Nature (London) **424**, 824 (2003).
[17] S. A. Maier and H. A. Atwater, J. Appl. Phys. **98**, 011101 (2005).
[18] L. Novotny, Phys. Rev. Lett. **98**, 266802 (2007).
[19] A. Alú and N. Engheta, Phys. Rev. Lett. **101**, 043901 (2008).
[20] P. Ghenuche, S. Cherukulappurath, T. H. Taminiau, N. F. van Hulst, and R. Quidant, Phys. Rev. Lett. **101**, 116805 (2008).
[21] M. L. Brongersma, J. W. Hartman, and H. A. Atwater, Phys. Rev. B **62**, R16356 (2000).
[22] S. A. Maier, P. G. Kik, and H. A. Atwater, Phys. Rev. B **67**, 205402 (2003).
[23] M. I. Tribelsky and B. S. Luk'yanchuk, Phys. Rev. Lett. **97**, 263902 (2006).
[24] J. B. Pendry, Phys. Rev. Lett. **85**, 3966 (2000).
[25] N. I. Zheludev, Nat. Mater. **7**, 420 (2008).
[26] M. Silveirinha and N. Engheta, Phys. Rev. Lett. **97**, 157403 (2006).
[27] K. Aydin, I. Bulu, and E. Ozbay, Appl. Phys. Lett. **90**, 254102 (2007).
[28] V. M. Shalaev, Nature Photon. **1**, 41 (2007).
[29] E. O. Kamenetskii, e-print arXiv:0909.4920.
[30] J. F. Nye and M. V. Berry, Proc. R. Soc. London A **336**, 165 (1974).
[31] A. Gurevich and G. Melkov, *Magnetic Oscillations and Waves* (CRC Press, New York, 1996).
[32] R. S. Elliot, *An Introduction to Guided Waves and Microwave Circuits* (Prentice-Hall Inc., New Jersey, 1993).
[33] M. V. Berry, R. G. Chambers, M. D. Large, C. Upstill, and J. C. Walmsley, Eur. J. Phys. **1**, 154 (1980).
[34] Y. Aharonov and D. Bohm, Phys. Rev. **115**, 485 (1959).
[35] F. Vivanco and F. Melo, Phys. Rev. E **69**, 026307 (2004).
[36] E. O. Kamenetskii, J. Appl. Phys. **105**, 093913 (2009).
[37] T. H. R. Skyrme, Proc. R. Soc. London A **260**, 127 (1961).
[38] C. M. Savage and J. Ruostekoski, Phys. Rev. Lett. **91**, 010403 (2003).